Meteoritics & Planetary Science 34, 949–958 (1999)

Airborne intensified charge-coupled device observations of the 1998 Leonid shower

IAN S. MURRAY[1], ROBERT L. HAWKES[1]* AND PETER JENNISKENS[2]

[1]Mount Allison University, Physics Department, 67 York Street, Sackville, New Brunswick E4L 1E6, Canada
[2]SETI Institute, NASA Ames Research Center, Mail Stop 239-4, Moffett Field, California 94035-1000, USA
*Correspondence author's e-mail address: rhawkes@mta.ca

(Received 1999 June 2; accepted in revised form 1999 August 17)
(Presented at a Workshop on the Leonid Multi-Instrument Aircraft Campaign, Moffett Field, California, 1999 April 12–15)

Abstract–We have used dual coaxial microchannel plate image-intensified monochrome charge-coupled device (CCD) detectors run at standard NTSC frame rates (30 frames per second, fps) to study the Leonid meteor shower on 1998 November 17 from an airborne platform at an altitude of ~13 km. These observations were part of NASA's 1998 Leonid multi-instrument aircraft campaign (MAC). The observing systems had fields of view (width) of 16.3° and 9.5°, and limiting stellar sensitivities of +8.3^m and +8.9^m. During 12 h of recording, 230 meteors were detected, of which 65 were Leonid meteors. Light curves are presented for 53 of these meteors. The magnitudes at peak brightness of the meteors investigated were generally in the range from +4.0^m to +6.0^m. The mass distribution indices for the two samples are 1.67 and 1.44, with the former being based on the wider field of view dataset. The light curves were skewed with the brightest point towards the beginning of the meteor trail. The *F* parameter for points one magnitude below maximum luminosity had a mean value of 0.47 for the wider field system and 0.37 for the more sensitive narrower field system. We provide leading and trailing edge light curve slopes for each meteor as another indication of light curve shape. There were few obvious flares on the light curves, indicating that in-flight fragmentation into a large number of grains is not common. There is variability in light curve shape from meteor to meteor. The light curves are inconsistent with single, compact body meteor theory, and we interpret the data as indicative of a two-component dustball model with metal or silicate grains bonded by a lower boiling point, possibly organic, substance. The variation in light curve shape may be indicative of differences in mass distribution of the constituent grains. We provide trail length *vs.* magnitude data. There is only a slight hint of a bend at +5^m in the data, representing the difference between meteors that have broken into a cluster of grains prior to grain ablation, and those that continue to fragment during the grain ablation phase. Two specific meteors show interesting light curve features. One meteor is nebulous in appearance, with significant transverse width. The apparent light production region extends for 450 m from the center of the meteor path. Another meteor has several main fragments, and evidence of significant separated fragments. We offer several suggestions for improvements for the 1999 Leonid MAC light curve experiment.

INTRODUCTION

Until *Stardust* and other planned cometary dust sample-and-return missions are successfully completed, we must infer the physical and chemical properties of cometary meteoroids indirectly from the details of their interaction with the Earth's atmosphere as meteors. This paper is concerned with how the spatial and temporal distribution of light production in the meteor can be used to establish the physical structure of meteoroids observed during NASA's 1998 Leonid multi-instrument aircraft campaign (MAC) (Jenniskens *et al.*, 1999). Our approach was to use light curves, plots of meteor luminous intensity with time, to suggest the structure and related parameters of the Leonid meteoroids. The physical structure of meteoroids is of both astrophysical and practical importance. Effects of interaction of meteoroids with spacecraft will be dependent upon the physical structure of the meteoroid (Hawkes *et al.*, 1998a; Correll *et al.*, 1999). Ceplecha *et al.* (1998) have reviewed the physics of meteor ablation.

Light is produced through atomic collisions between ablated meteoric atoms and atmospheric atoms. The light produced by a meteor (except in the case of large meteoroids) is assumed approximately proportional to the rate of change in its kinetic energy (and because the velocity does not change significantly over the luminous trail of a small meteor, this is proportional to the rate of change of mass). Because the atomic excitation and decay process is rapid, the light produced gives a direct indication of the instantaneous rate of ablation. The dimensions of the meteoroids studied in this work (typically hundreds of microns) are much less than the mean free path at the heights of atmospheric ablation, and therefore the interaction between the atmosphere and the meteoroid is essentially molecular, with no air cap or shock wave formation.

A solid, compact, nonfragmenting meteoroid should produce a classical light curve with the point of maximum luminosity near the end (McKinley, 1961). For some time, there has been compelling evidence that most meteoroids in the size regime studied by visual, photographic, and television techniques have a composite dustball structure. The indication that these meteoroids were not strong, compact stones similar in structure to meteorites came from the fact that the light trails were statistically shorter than expected for solid compact objects, some demonstrated flares indicative of in-flight fragmentation, a number demonstrated wake from separated grains, and most of the light curves did not have the shape expected for single body ablation. A quantitative model for the ablation of dustball meteors (Hawkes and Jones, 1975) pictures the meteoroids as composed of silicate and metallic grains bonded by a second component of lower boiling point. We will consistently refer in this paper to these subunits of the overall meteoroid as grains and reserve the word meteoroid for the entire solid object. Several authors (Hapgood *et al.*, 1982; Beech, 1984, 1986) have successfully applied this model to different cometary meteor showers.

It is possible that the component responsible for the bonding of the grains is primarily organic in nature and similar to the CHON particles detected during the P/Comet Halley spacecraft observations in 1986. The organic component might produce little luminosity in the visual and near-visual regions of the spectrum and might well be undetected (the majority of meteor luminosity is due to excitation lines from the metallic grains). Recently, it has been postulated (Steel, 1998; Elford *et al.*, 1997) that the organic component may be very abundant in Leonid meteors. If true, this would mean that the space impact hazard is significantly underestimated.

As previously mentioned, single nonfragmenting meteoroid ablation would produce light curves that have the point of maximum luminosity near the end. However, faint television meteors have been found to have light curves that vary from meteor to meteor, but which are on average nearly symmetric, and with few flares (Benyukh, 1974; Hawkes *et al.*, 1987; Fleming *et al.*, 1993; Campbell *et al.*, 1999). This has been interpreted in terms of the two-component dustball model as due to the fact that many of these meteors are clustered into constitutent grains prior to grain ablation, and a distribution in the masses of the grains results in an overall light curve that is broader and skewed toward the beginning from that due to any single grain size (Campbell, 1998; Campbell *et al.*, 1999). It was found that a grain mass range from 10^{-6} to 10^{-12} kg was needed to model Leonid and Perseid meteors. It was the goal of this study to expand the observational dataset for this conclusion, and to use two cameras of different spatial resolution to seek other indicators of meteoroid physical structure.

EXPERIMENTAL OBSERVATIONS

Observations were made using two coaxial microchannel plate (MCP) second-generation intensified charge-coupled device (CCD) camera systems (S-20 spectral response—sensitive from near IR to near UV but mainly concentrated in visual). One camera (which we have designated M) was equipped with a 50 mm/f0.95 objective lens providing a field of view of 16.3 × 12.0°, a limiting sensitivity of +8.3 apparent stellar magnitude, and a spatial resolution of 1.5'. The second camera (designated N) used an 85 mm/f2.0 objective lens resulting in a field of view of 9.5 × 7.3°, a limiting sensitivity of +8.9 apparent stellar magnitude, and spatial resolution of 0.9'. Both

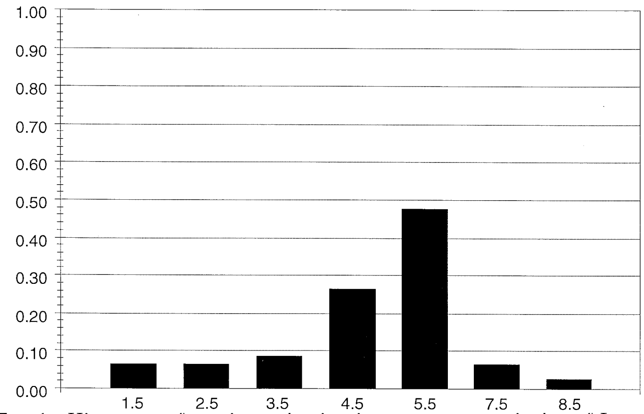

FIG. 1. Histogram of maximum luminosity apparent magnitudes of Leonid meteors analyzed (cameras M and N combined). Vertical axis is the fraction of the sample, whereas the horizontal axis is the astronomical magnitude at peak luminosity.

systems were mounted at a constant elevation angle of 75° that pointed out of a right side (61°) optical glass window onboard the flying infrared signature technology aircraft (FISTA). The FISTA flew a pentagonal path off the coast of Okinawa, Japan. Global positioning system (GPS) data and aircraft heading, altitude, pitch, and yaw were recorded during flight; and with this information, the camera direction during each leg was ascertained. Video was recorded onto NTSC standard VHS tapes and a time/date stamp was added to each. A total of 12 h of data was recorded and 230 meteors were detected during peak night on 1998 November 17. The distribution of meteor astronomical magnitudes at maximum luminosity is shown in Fig. 1, with the majority of the meteors having a maximum brightness in the range +4 to +6. The meteor images were digitized using a SCION LG-3 card at 29.97 frames per second (fps) rate and analyzed using NIH Image v1.61 software on a Power Macintosh 9600/233 computer. Images are saved in an uncompressed TIFF (640 × 480 × 8 bit) format for analysis.

PHOTOMETRIC PROCEDURE

Photometric calibrations were performed for both camera systems and for three different times during the night. The

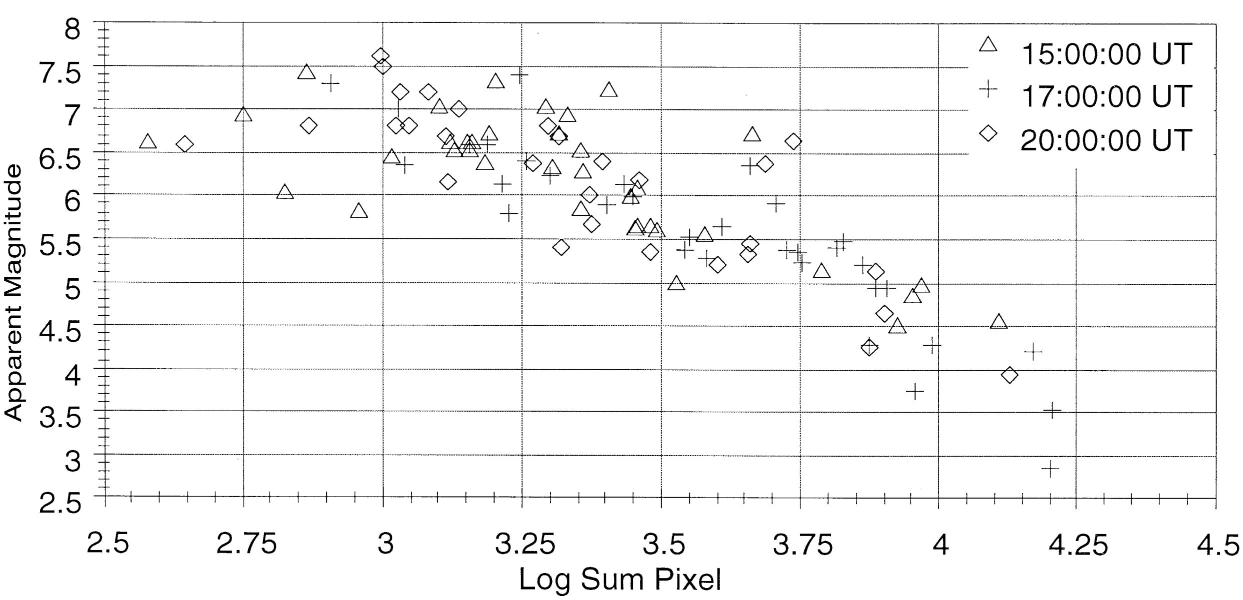

FIG. [illegible] ground subtra[illegible]

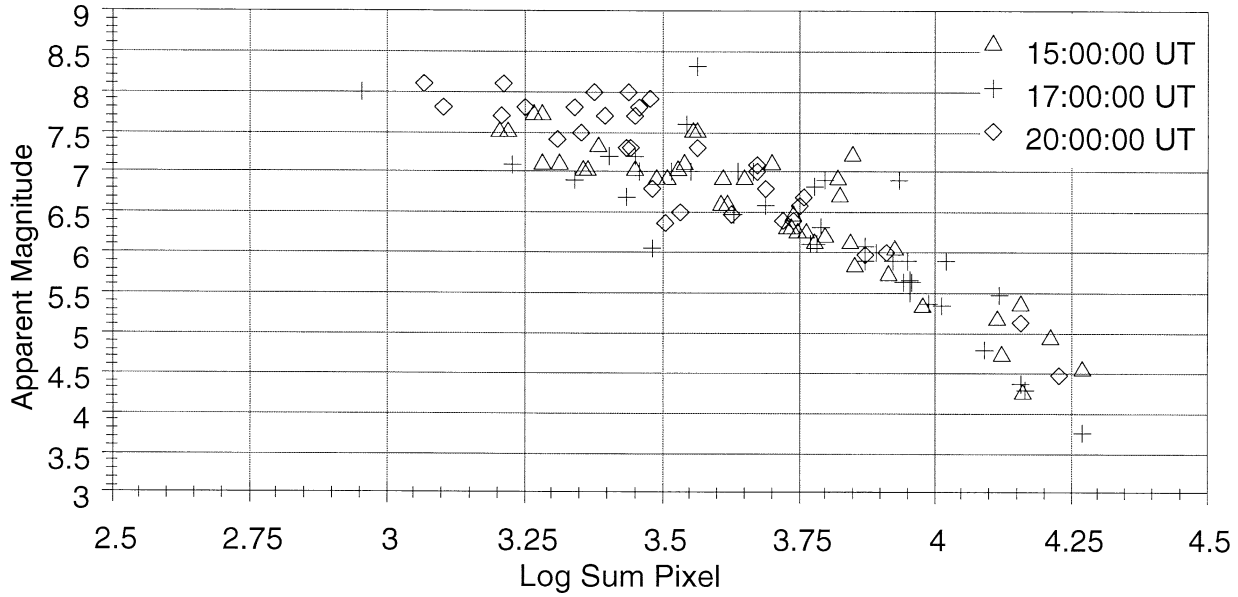

FIG. 3. Photometric calibration plot (magnitude *vs.* the logarithm of the summation of the intensity over the stellar image, with regional background subtracted) for the 85mm/f2.0 camera N.

procedure used was developed by Hawkes *et al.* (1993), and used for study of shower meteor light curves by Fleming *et al.* (1993) and Campbell *et al.* (1999). The log sum pixel technique uses the summation of the relative pixel intensities minus the local background intensity over an ROI (region of interest), which includes all of the intensity from the meteor or reference star being measured. A series of reference stars are identified, their absolute magnitude and log sum pixel values are recorded. Calibration plots (Figs. 2 and 3) are computed and a linear regression is performed between the log sum pixel values and the astronomical magnitude of the reference stars. This allows for the magnitude of each measured point along a meteor's path to be determined. One limitation of this procedure is that it only works well for those meteors that have similar magnitude reference stars. Therefore, it is difficult to determine the precise photometry for bright or very faint meteors. With the apparent magnitude values, it is possible to calculate photometric masses for each meteor by integrating the light curve,

$$m_p = \frac{2}{v^3 \tau_o} \int I \, dt$$

In the preceding equation, m_p represents the photometric mass, v is the velocity of the meteoroid (assumed approximately constant over most of the visible part of the trajectory and, therefore, taken out of the integration), and I is the luminous intensity of the meteor. The luminous efficiency factor is not at all well known for fast meteors. In deriving the above equation, we have assumed that the dependence of luminous efficiency factor on velocity is a linear one. If we express the luminous intensity I in terms of a number of 0 magnitude stars to produce an equivalent intensity, then the constant τ_o has the value 1.0×10^{-10}, assuming that all other quantities have been expressed in SI units (this is based on the Verniani, 1965, determination of luminous efficiency factor).

SYMMETRY OF LIGHT CURVES

Discrimination of Leonid meteors was performed using a test for radiant match and apparent velocity. A number of meteors proved to be too faint for analysis, but photometric light curves were plotted for 45 Leonid meteors from camera M and 20 Leonid meteors from the camera N. From these, a few were found to have significantly incomplete light curves and were omitted from further study. The sequence of light curves in Figs. 4 and 5 are drawn on a relative scale (both in intensity and in time) to show their overall shapes. Very few flares were apparent and many of the light curves were skewed left or symmetric in shape. The relative absence of flares is consistent with the results of the study of Perseid and Leonid light curves by Campbell *et al.* (1999).

A statistical analysis was performed using a modified set of F parameters—the ratio of the distance to the point of maximum brightness to the entire length of the curve—to specify the skew of the light curves (Fleming *et al.*, 1993),

$$F_{\Delta m} = \frac{t_{B\Delta m} - t_{MAX}}{t_{B\Delta m} - t_{E\Delta m}}$$

In this equation, F is the skew parameter for the light curve, with a value in the range from 0 to 1. A low value is indicative of a light curve that is skewed with a maximum luminosity point towards the beginning. In the notation of the preceding equation, t_B, t_E, and t_{MAX} represent the time for beginning, ending, and maximum luminosity for various magnitude intervals Δm. The F values were calculated for magnitude intervals Δm of 0.25, 0.50, 0.75, 1.0, and 1.25 fainter than maximum luminosity, as was done by Fleming *et al.* (1993). The F-value distributions are shown in Figs. 6 and 7. The 85 mm cameras system showed a mean of 0.38 for its five intervals of F values, which corresponds to a left skewed trend for the 16 relatively complete light curves (Fig. 7). The other system proved to be much more symmetric, averaging 0.47 for the F values, and calculated for 37 relatively complete light curves (Fig. 6; see Table 1 for details).

In past light curve studies, other means of determining skewness have been defined (Campbell, 1998; Campbell *et al.*, 1999) to aid in cases when F values are not indicative of the observed trend. Here, we have used leading and trailing slopes of the best fit lines through each edge's data points to the point of maximum. Slopes are expressed in term of log sum pixel per seconds. A summary of

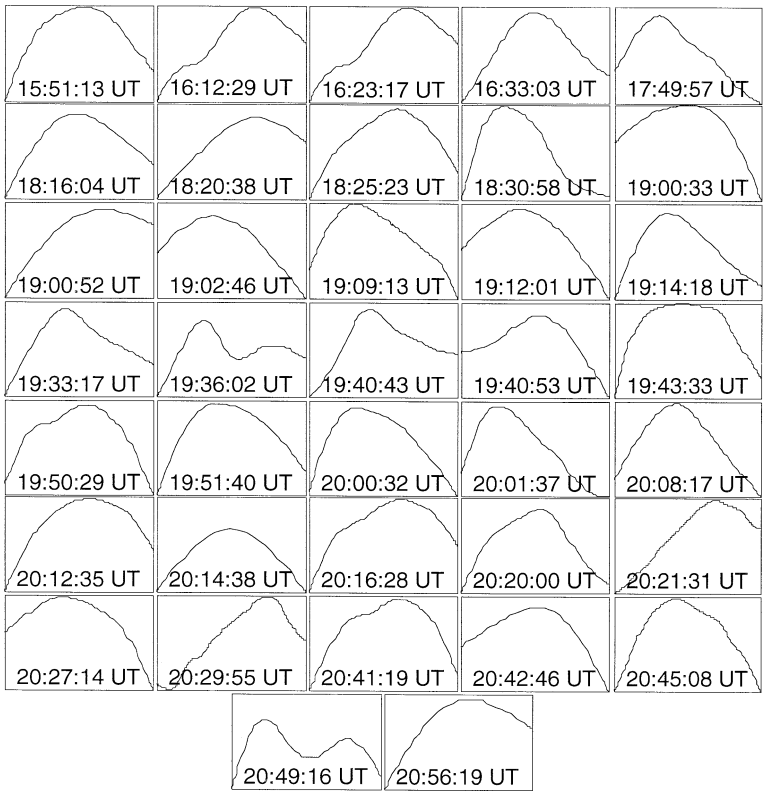

FIG. 4. Photometric light curves for Leonid meteors observed with camera system M (50 mm objective lens). The vertical axis is a relative scale proportional to magnitude, whereas the horizontal axis is a relative time scale. The purpose of this plot is to demonstrate shapes, not absolute values, of the light curves. The curves shown are smooth fits to the data points, with actual data at discrete 0.033 s time steps.

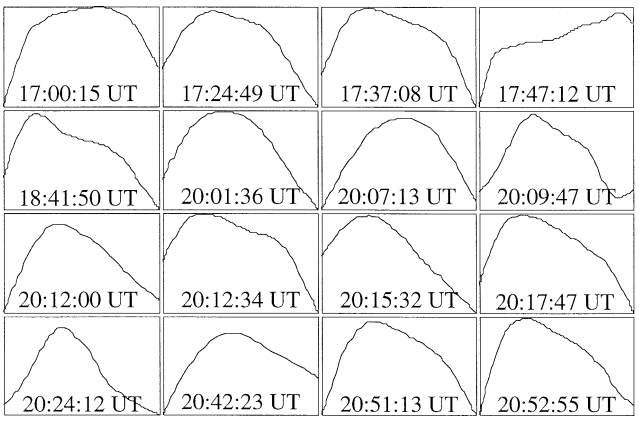

FIG. 5. Photometric light curves for Leonid meteors observed with camera system N (85 mm objective lens). The vertical axis is a relative scale proportional to magnitude, whereas the horizontal axis is a relative time scale. The curves shown are smooth fits to the data points, with actual data at discrete 0.033 s time steps.

individual F values (averaged over the various magnitude intervals) and the corresponding leading and trailing slopes are found in Tables 2 and 3.

It is highly significant that most of the light curves are inconsistent with nonfragmenting single body ablation theory, in that they are skewed towards the beginning of the light curves or nearly symmetric. This point will be returned to in the discussion.

For those meteors that were determined to be Leonids, it was possible to determine the atmospheric trajectory trail length (we exclude meteors with a significant portion of the light curve outside the field of view). The trail length is determined from the number of video frames and the assumed geocentric velocity (71.3 km/s) of the shower. Trail lengths are another indication of physical structure, because fragmenting dustball meteors would be expected to have shorter trail lengths than single compact objects of the same total trail length (Jones and Hawkes, 1975). Also, the dependence of trail length and heights with mass can be used to determine the thermal properties of the bonding substance holding the meteoroid grains together. This technique was used by Hapgood *et al.* (1982) and Beech (1984, 1986) for other meteor showers. However, because of the small size of the data sample, and the wide variation in zenith angle over the recording period, no clear trend was apparent in the Leonid trail length data.

MASS DISTRIBUTION

Although the primary goal of this experiment was to study the light curves of Leonid meteors and the implications for meteoroid physical structure, with the photometric masses already determined the mass distribution for the shower could readily be determined. It is generally assumed that the distribution of number of meteors of different masses in a meteor shower is given by the following relationship:

$$dN = Cm^{-s}\, dm$$

where dN is the number of meteoroids with mass between m and $m + dm$. The larger the s value, the more dramatic is the increase in meteor number as one goes to smaller masses. Sporadic meteors generally have s values of ~2.0, whereas each shower has a characteristic s value (generally in the range 1.4 to 2.0). The 1997 Leonid shower had an s value of ~1.7 on peak night (Hawkes *et al.*, 1998b), and this value was approximately constant over systems of varying sensitivity. The 1996 Leonid shower had an s value of 1.64, according to Brown *et al.* (1998).

In actually computing the mass distribution index, one uses the integrated form of the above equation and determines the slope of a plot of logarithm cumulative number *vs.* logarithm of photometric mass. Mass distributions were plotted separately for each camera system used in our study. The sample sizes were relatively small in both cases, 37 meteors for the 50 mm system and 16 meteors for the 85 mm system. These data are shown in Figs. 8 and 9. The mass distribution index s had a value of 1.67 from the larger sample size (50 mm focal length objective lens), and the second system (85 mm focal length objective lens) yielded an s value of 1.44. Considering the very small sample size, these numbers should be interpreted as

TABLE 1. Mean F values for magnitude intervals.

Camera system		$F_{0.25}$	$F_{0.50}$	$F_{0.75}$	$F_{1.00}$	$F_{1.25}$
50 mm (M)	Mean	0.46	0.45	0.48	0.47	0.49
	Std. Dev.	0.20	0.18	0.14	0.15	0.14
85 mm (N)	Mean	0.41	0.39	0.37	0.37	0.37
	Std. Dev.	0.19	0.16	0.15	0.15	0.16

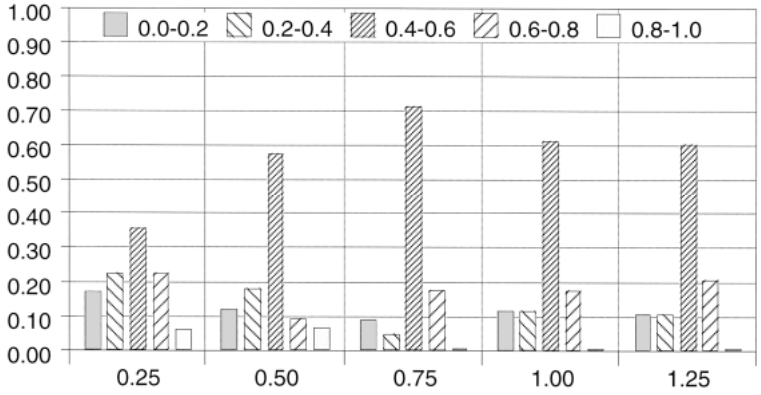

FIG. 6. The F-value distribution histogram for the Leonid meteors for five Δm intervals of the M camera system. Vertical axis is the fraction of the sample with a given F value, with the histogram based upon a division of the data into five equal intervals in F value covering the range from 0 to 1. The different groups are for different magnitude difference intervals over which the F value is measured. For example, for points 1 magnitude fainter than maximum luminosity, 61% of the observed meteors have F values in the range from 0.4 to 0.6.

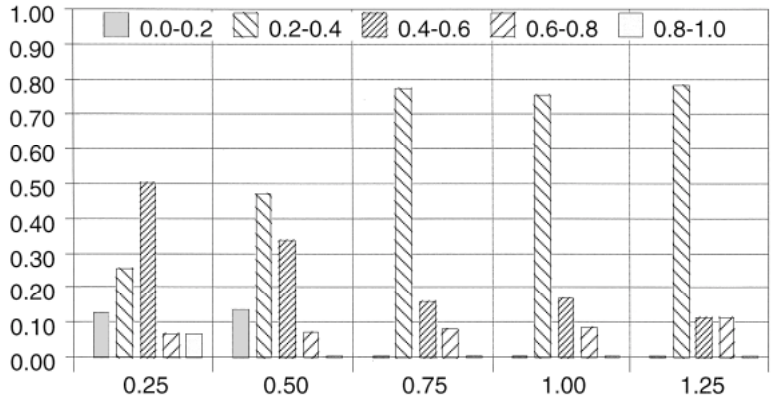

FIG. 7. The F-value distribution histogram for the Leonid meteors for five Δm intervals of the N camera system. Vertical axis is the fraction of the sample with a given F value, with the histogram based upon a division of the data into five equal intervals in F value covering the range from 0 to 1. The different groups are for different magnitude difference intervals over which the F value is measured. For example, for points 1 magnitude fainter than maximum luminosity, 75% of the observed meteors have F values in the range from 0.2 to 0.4.

tentative. Early analysis of the 1998 Leonid shower from other observers (Brown, pers. comm.) indicates that the *s* value varied from the very low value of ~1.25 one night prior to maximum up to ~1.75 at the time of the predicted maximum flux (~19:00 UT on 1998 November 17). These observations are centered around that time, and therefore the values obtained, particularly from the larger sample set, are consistent with other work. For the same night, Correll *et al.* (1999) found from ground-based similar electro-optical equipment in Mongolia a *s* value in range 1.3–1.7. This also is a preliminary value based on a small subset of the entire data gathered by that group. Visual data has perhaps provided the most complete picture yet of *s* values for the 1998 Leonids. Arlt (1998) has found a value of 1.4 for the population index on 1998 November 16/17, and 2.0 for November 17/18, which would correspond to *s* values of 1.36 and 1.75.

NEBULOUS METEOR

At 17:47:12 UT on 1998 November 17, an unusual meteor with a nebulous appearance was detected by camera N. A time sequence for this meteor is shown in Fig. 10. The light production region for this meteor has considerable transverse (to motion of the meteor) spread that is not characteristic of most other meteors detected of similar brightness (in the bottom line of Fig. 10 is a comparison meteor of similar brightness). At the time of detection, the aircraft was on a course heading of 230° and was flying at a height of 13 km. Some image processing was performed to eliminate first artifacts from the intensifier or CCD. A sequence of frames immediately prior to the meteor was digitized and averaged to establish a background that was subsequently subtracted from each video frame containing the meteor.

Although observations were only available from a single station, approximate heights could be determined using the angular velocity information provided by the video record. A check indicated that the meteor direction and apparent speed were consistent with the Leonid shower. A Leonid radiant of α = 153° and δ = 22° was assumed, along with a geocentric velocity of 71.3 km/s. The meteor was first observed at a height of 138 km and a range of 155 km. The meteor had a luminosity of $+1.6^m$ in the portion of the trail pictured (the meteor was increasing in brightness as it left the field of view—the slight dip shown in the light curve of Fig. 3 for this meteor is an instrumental effect of the edge of the field of view—and a wider field camera from the campaign recorded a later maximum brightness of –4 magnitude for this meteor). The average distance from the main body of ejected material was measured to be 450 m from each side and is seen clearly on frame 11 from Fig. 10. For very bright meteors, blooming (a result of pixel saturation) and persistence can slightly widen the meteor's image. Yet a sharp drop in pixel intensities is still prevalent when compared to the background, and this is expected for most meteor images. A cross-sectional intensity profile was plotted for both this meteor and a comparison meteor of comparable brightness in Fig. 11. In the case of the nebulous meteor, a much broader curve with irregulatities is observed and indicative of ablating material outside the main body.

FRAGMENTING METEOR

At 20:12:34 UT on 1998 November 17, a meteor was detected by camera N in which in-flight fragmentation and some longitudinal spread of major fragments is apparent. At the time of detection, the aircraft was on a path heading 350.8° and at an altitude of 13 km. Similar image processing was performed as mentioned in the previous section to eliminate first-order system noise (see Fig. 12 for a sequence for this meteor). Also, the same single station analysis technique was used to determine range and height. The meteor was first observed at a height of 125 km and at a range of 129 km . A computed maximum luminosity of $+4.8^m$ was calculated. A section separated from the main body of the meteor in frame 11 (Fig. 12). This portion was measured to be 190 m in length and separated by 560 m from the main section of the meteor. Profile plots for this meteor are shown in Fig. 13 and clearly indicate the presence of several main luminosity regions corresponding to multiple fragments. To produce the very sharply defined and strongly lagged brief intensity peak would require the presence of very small grains. We have modeled the atmosphere at the height of this meteor fragment (114 km), solving ablation equations similar to those developed by Fyfe and Hawkes (1986) and found that one requires grains on the

TABLE 2. Camera M (50mm/f0.95)) photometric results.*

Time UT	Maximum luminosity (0^m)	Photometric mass (kg)	$F_{average}$	$Slope_{leading}$	$Slope_{trailing}$	*B*	*M*	*E*
15:51:39	4.1	1.9×10^{-7}	0.49	9.6	–7.1	0	1	1
16:12:29	4.8	8.7×10^{-8}	0.61	8.5	–8.4	1	1	0
16:23:17	1.8	1.7×10^{-6}	0.64	8.0	–6.3	0	1	0
16:33:03	4.8	1.0×10^{-7}	0.48	5.9	–4.3	1	1	1
17:49:57	4.8	1.0×10^{-7}	0.54	4.5	–3.3	1	1	1
18:16:04	5.3	3.7×10^{-8}	0.19	16.6	–5.1	1	1	1
18:20:38	6.0	1.9×10^{-8}	0.49	9.5	–7.6	1	1	1
18:25:23	3.1	4.5×10^{-7}	0.48	7.7	–7.7	1	1	1
18:30:58	5.3	7.3×10^{-8}	0.17	9.1	–2.1	0	1	1
19:00:33	5.0	7.5×10^{-8}	0.57	2.5	–6.1	1	1	1
19:00:52	5.2	4.1×10^{-8}	0.52	13.4	–6.2	1	1	1
19:02:46	5.6	2.5×10^{-8}	0.40	10.5	–9.9	1	1	1
19:09:13	4.1	2.6×10^{-7}	0.43	6.5	–4.2	1	1	1
19:12:01	5.4	4.3×10^{-8}	0.50	7.4	–10.1	1	1	1
19:14:18	5.0	5.5×10^{-8}	0.20	18.4	–5.6	1	1	1
19:33:17	5.5	5.6×10^{-8}	0.53	7.1	–3.3	1	1	1
19:36:02	5.5	4.1×10^{-8}	0.60	12.0	–2.2	1	1	1
19:40:43	6.1	4.2×10^{-8}	0.27	4.4	–1.4	1	1	1
19:40:53	5.5	4.1×10^{-8}	0.43	4.1	–7.9	1	1	1
19:43:33	2.5	1.4×10^{-6}	0.47	7.7	–5.8	1	1	1
19:50:29	5.5	5.4×10^{-8}	0.47	4.8	–6.0	0	1	1
19:51:40	4.4	1.1×10^{-7}	0.15	19.6	–4.8	1	1	1
20:00:32	4.9	6.5×10^{-8}	0.13	26.5	–6.9	1	1	1
20:01:37	5.1	8.3×10^{-8}	0.20	8.3	–2.5	1	1	1
20:08:17	4.4	1.2×10^{-7}	0.68	7.4	–8.6	1	1	1
20:12:35	3.8	3.0×10^{-7}	0.50	6.8	–5.0	1	1	1
20:14:38	5.5	2.2×10^{-8}	0.50	11.3	–11.4	1	1	1
20:16:28	4.8	1.1×10^{-7}	0.45	6.6	–4.7	1	1	1
20:20:00	5.3	4.6×10^{-8}	0.73	6.6	–9.5	1	1	1
20:21:31	2.2	1.7×10^{-6}	0.52	5.0	–3.6	1	1	0
20:27:14	5.1	8.4×10^{-8}	0.35	4.4	–5.2	1	1	0
20:29:55	3.0	7.9×10^{-7}	0.60	4.0	–5.7	1	1	1
20:41:19	5.7	4.5×10^{-8}	0.50	5.9	–6.9	1	1	1
20:42:46	5.7	2.8×10^{-8}	0.82	4.6	–17.5	1	1	1
20:45:08	4.5	2.1×10^{-7}	0.49	5.1	–3.9	1	1	1
20:49:14	5.7	3.9×10^{-8}	0.28	10.0	–1.4	1	1	1
20:56:19	5.9	2.2×10^{-8}	0.67	12.3	–9.0	1	1	1

*Maximum luminosity is the brightest recorded point, expressed in astronomical magnitudes. Photometric mass is based on an integration over the observed light curve and is expressed in kilograms. The skew parameter *F* is an average over the five computed values for that meteor. The next two columns give the slope of the logarithm of the intensity *vs.* time for the portion of the light curve before and after maximum luminosity. The final three columns indicate if the *B* (beginning), *M* (maximum luminosity), and *E* (ending) point of a meteor trail occurs in (1) or outside (0) the field of view.

order of 10^{-16} to 10^{-17} kg, assuming that the grain density is 3400 kg m^{-3}. This is considerably smaller than the grains usually reported (*e.g.*, Campbell *et al.*, 1999; Simonenko, 1968). We plan to extend modeling of the details of the light curves in a subsequent paper.

DISCUSSION

We have found that the light curves for the Leonid meteors investigated in this experiment are approximately symmetrical, with a slight skew towards the beginning. This means that Leonid meteoroids in the size range studied here (10^{-5} to 10^{-8} kg) cannot be single compact objects. Classical meteor theory (McKinley, 1961; Öpik, 1958), no matter what the meteoroid bulk density and thermal parameters, will lead to late skewed meteor light curves with any reasonable atmospheric density profile. We show in Fig. 14 a light curve for a single-object 10^{-5} kg Leonid meteor with a cosine of zenith angle of 0.7. Although the details of the heights and trail lengths can be adjusted with changes in the thermal and density parameters, the light curves will always be skewed towards the ending point for single compact nonfragmenting meteoroids. For example, for a 1.0 magnitude luminous difference, the single compact body theoretical *F* value is ~0.65. One can obtain symmetric and early skewed light curves with the two-component dustball model (Hawkes and Jones, 1975) if one assumes that there is a mixture of grain sizes (Campbell, 1998; Campbell *et al.*, 1999). It was found in these studies that one needed grains between 10^{-6} and 10^{-12} kg in order to model the 1997 Leonid meteors. It is not clear whether the anomalously high Leonids reported by Fujiwara *et al.* (1998) may be evidence of disintegration of the component that bonds the meteoroid.

There is significant variation in light curve shape from meteor to meteor. This could be indicative of either a difference in grain size distribution or the presence of some meteors that had not been pre-clustered into constituent grains prior to commencement of ablation of the grains themselves (see Hawkes and Jones, 1975). Although

TABLE 3. Camera N (85mm/f2.0) photometric results.*

Time UT	Maximum luminosity (0^m)	Photometric mass (kg)	$F_{average}$	$Slope_{leading}$	$Slope_{trailing}$	*B*	*M*	*E*
17:00:15	2.1	1.4×10^{-6}	0.79	6.0	–11.4	0	1	0
17:24:49	4.7	9.4×10^{-8}	0.39	8.9	–7.1	1	1	0
17:37:08	1.6	2.0×10^{-6}	0.36	5.9	–3.9	0	1	0
17:47:12	1.7	1.9×10^{-6}	0.51	3.1	–7.1	0	1	0
18:41:50	4.4	1.6×10^{-7}	0.42	7.6	–3.3	0	1	1
20:01:36	6.5	1.5×10^{-8}	0.49	11.6	–11.8	0	1	1
20:07:13	5.6	3.4×10^{-8}	0.46	6.9	–6.4	1	1	1
20:09:47	5.8	4.1×10^{-8}	0.21	6.9	–3.2	0	1	1
20:12:00	5.5	3.2×10^{-8}	0.20	17.2	–5.2	1	1	1
20:12:34	4.8	9.9×10^{-8}	0.38	8.4	–6.2	1	0	1
20:15:32	7.1	1.3×10^{-8}	0.30	3.4	–2.1	1	1	1
20:17:47	5.1	8.2×10^{-8}	0.36	9.0	–3.4	1	1	1
20:24:12	5.5	5.1×10^{-8}	0.34	5.7	–3.4	1	1	1
20:42:23	6.3	1.7×10^{-8}	0.24	9.5	–3.0	1	1	1
20:51:13	4.7	9.2×10^{-8}	0.32	11.3	–3.0	1	1	1
20:52:55	3.5	3.6×10^{-7}	0.25	13.9	–4.3	1	1	1

*Maximum luminosity is the brightest recorded point, expressed in astronomical magnitudes. Photometric mass is based on an integration over the observed light curve and is expressed in kilograms. The skew parameter *F* is an average over the five computed values for that meteor. The next two columns give the slope of the logarithm of the intensity *vs.* time for the portion of the light curve before and after maximum luminosity. The final three columns indicate if the *B* (beginning), *M* (maximum luminosity), and *E* (ending) point of a meteor trail occurs in (1) or outside (0) the field of view.

our plot of trail length *vs.* magnitude did not indicate a clear differentiation between still fragmenting and preclustered meteors, we believe this is due to the small sample size and the bias against long meteors by the narrow fields of view of the observing system. There is some hint that the trail length is relatively independent of meteoroid size for meteors fainter than +5 magnitude, which indicates that meteors smaller than this size are completely clustered prior to atmospheric ablation of the constituent grains.

The nebulous and fragmented meteoroids provide clear evidence for fragmentation of the Leonid meteoroids. Conventional theory is that small, high meteors have a light production region that is no more than meters in dimension. This is based on the argument that the atmospheric mean free path at typical Leonid ablation heights (105–125 km) is on the order of 1 m, which is orders of magnitude greater than the physical dimensions of the meteoroid. In the case of the nebulous meteor, light is produced from a region up to 450 m from the center of the meteor trail. Although part of this may be due to image blooming in the intensifier and/or CCD detector, clearly this meteor is significantly wider than other meteors of comparable brightness observed with the same equipment, and the real width of the light production region must be on the order of hundreds of meters. Without an air cap or shock wave phenomena, it is not clear what mechanism can separate material so widely transverse to the motion of the meteor. One possibility is that this particular meteor was preclustered in interplanetary space, and what we are witnessing is really a number of closely spaced meteoroid fragments (Piers and Hawkes, 1993). The appearance of jet-like features on bright Leonid meteors, and speculation regarding their possible nature, has recently been announced (LeBlanc *et al.*, pers. comm.).

The fragmented meteor is indicative of at least several fragments with clear separation along the line of motion of the meteor. Wake is a frequent phenomena for brighter meteors and a similar phenomena is likely here, in which grains of different sizes are aerodynamically separated during flight. The one sharp feature with significant deceleration from the meteor head is indicative of the presence of

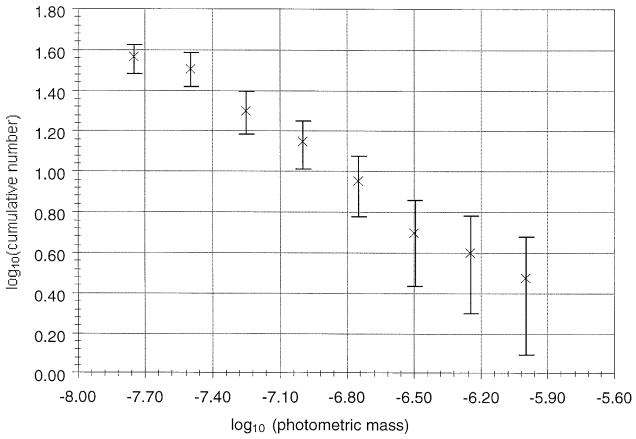

FIG. 8. Mass distribution plot for Leonid meteors observed with the M camera system. Log cumulative number of meteors *vs.* the logarithm of the photometric mass, expressed in kilograms.

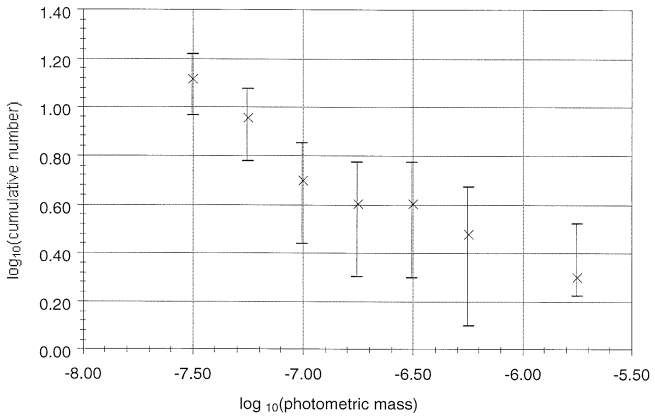

FIG. 9. Mass distribution plot for Leonid meteors observed with the N camera system. Log cumulative number of meteors *vs.* the logarithm of the photometric mass, expressed in kilograms.

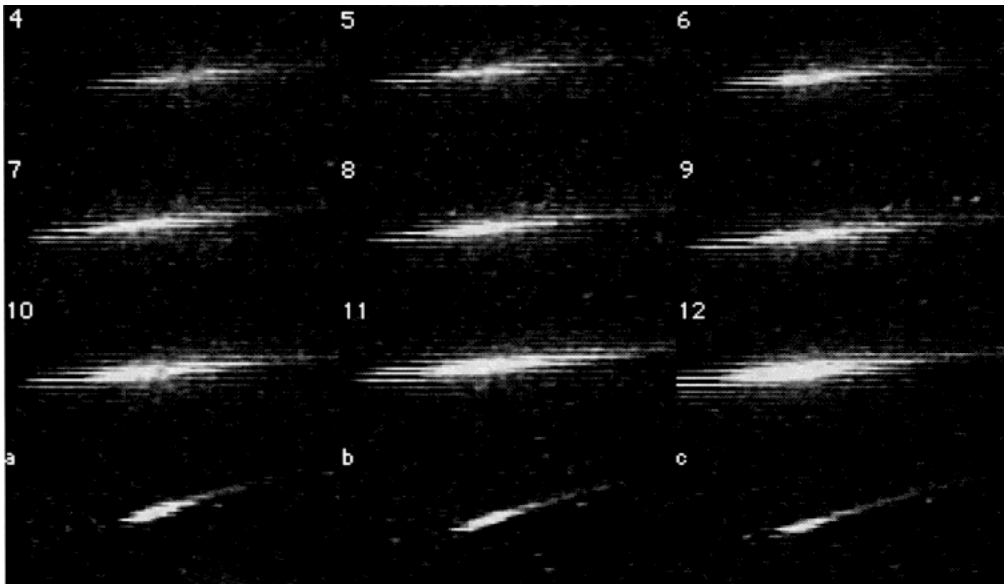

FIG. 10. Nebulous meteor, 17:47:12 UT 1998 November 17. This time sequence (0.03337 s between frames) shows frames 4 through 12 compared to a similar brightness reference meteor (frames a, b, c) of a later time, 18:48:13 UT. An average background was subtracted from each frame to reduce first-order intensifier noise and eliminate most stellar features.

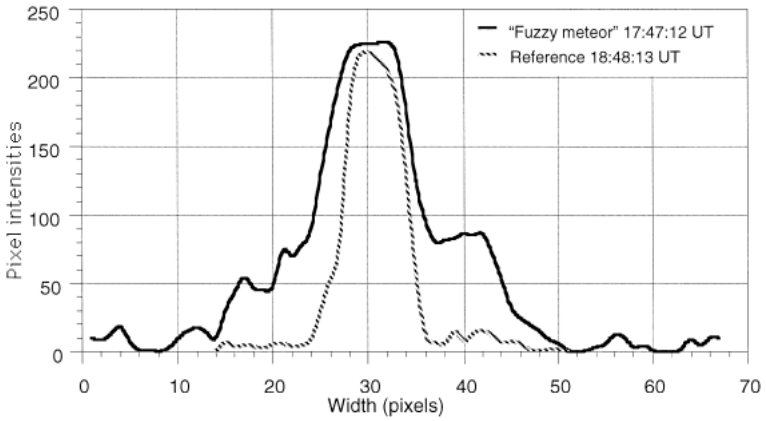

FIG. 11. Cross-sectional profile plots for frame 11 of the nebulous meteor and image *b* of the reference meteor. A smoothing routine was applied in addition to the background subtraction on both images in this case to eliminate odd field lines from producing false intensity levels .

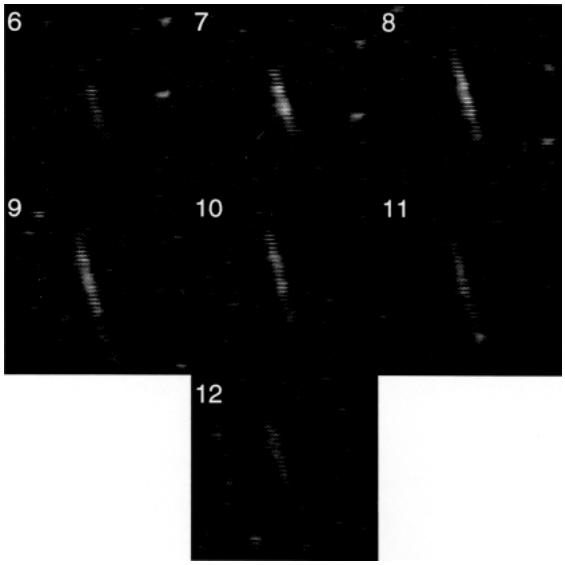

FIG. 12. Fragmenting meteor, 20:12:34 UT 1998 November 17. This time sequence (0.03337s) corresponds to frames 6 through 12 of the meteor in question. This image has an average background subtracted for elimination of first-order system noise. Frame 11 shows evidence of a rapid deceleration of grains.

very small grains within the meteoroid, probably on the order of 10^{-16} to 10^{-17} kg. If further modeling confirms this result, these will be the smallest grains reported for cometary meteors.

The light curve experiment was successful in observing a number of features related to the physical strength and structure of Leonid meteoroids. In a broad sense, the two-component organic (or other nonluminous material with relatively low boiling point) plus silicate/metallic grains model was supported, and it was shown that a grain size distribution is needed in order to model light curves. The airborne platform proved to be well adapted to light curve studies of meteors. Not only were clear skies guaranteed, but also the slight change in transparency from hour to hour for ground-level observations was removed. For the fields of view and resolutions of our cameras, aircraft motion proved not to be a significant difficulty. The stellar background provides a ready check for motion that may have contaminated a particular meteor trail. However, longer focal length optics would have much more serious problems.

Prospects are good for an equal or stronger Leonid shower in 1999. Based on the NASA 1998 Leonid MAC experience, we would propose some alteration to the light curve experiment. The coaxial nature of the experiment was less successful than anticipated partly because of problems with in-flight alignment and partly due to the different fields of view of the systems. We propose for 1999 two cameras that are coaxial and nominally identical, along with a mechanism for fine tuning the pointing of one camera relative to another. Also, we propose to line couple the two cameras so that each camera starts a new image at the identical point in time. With these changes, we anticipate being able to more fully investigate the reality of small features on the light curves using correlation

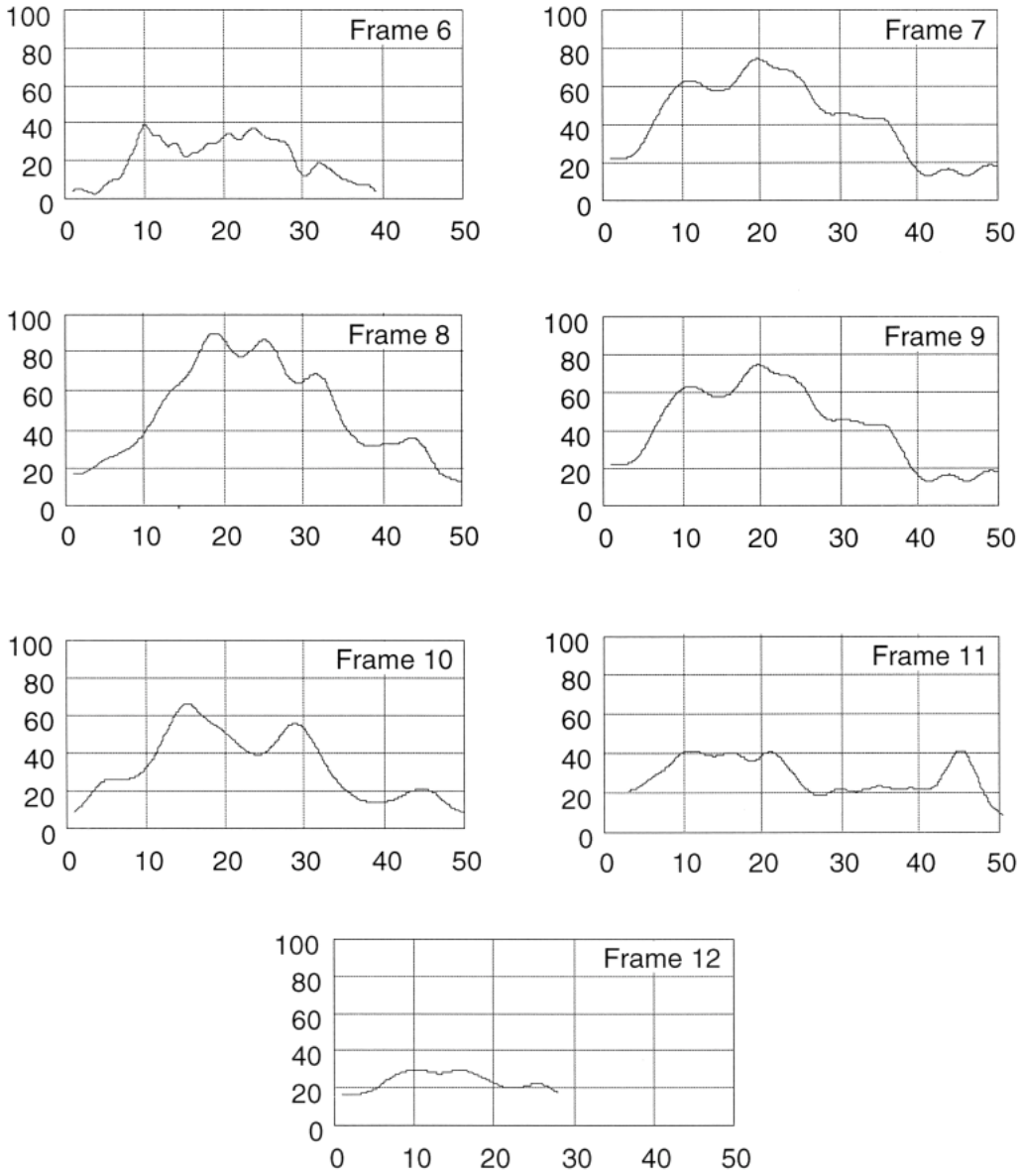

FIG. 13. Longitudinal profile plots of relative intensity for the sequence in Fig. 12. Here again smoothing and background subtraction was applied to each frame. Plotted is the relative intensity on the digitized image *vs.* distance along the trail (distances are expressed in image pixels), and the intensity scale is arbitrary.

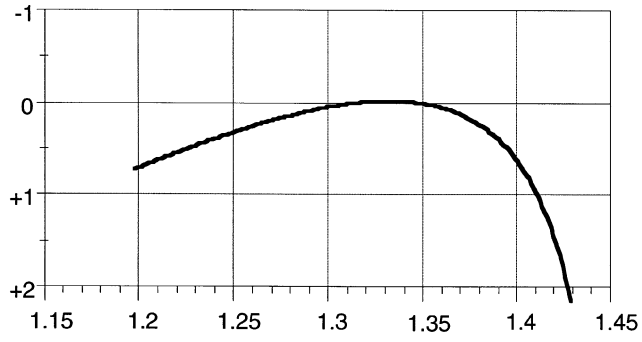

FIG. 14. Theoretical plot of magnitude *vs.* time (time is in seconds, but the absolute value is not significant) for a 10^{-5} kg Leonid meteoroid entering at a cosine of zenith angle value of 0.7. No fragmentation is assumed, and the meteor is classical with a light curve skewed towards the end of the light trail.

techniques. A third coaxial, but much wider field of view, observing system would be helpful to distinguish which part of the light curve is under investigation (and also to ease identification of the fields being viewed). With sufficient funding, a higher resolution system (or one with a gated image intensifier) would be valuable in helping to answer questions regarding the physical nature of Leonid meteors. Also, a system with a better dynamic range, corresponding to 12 bits or more of intensity information, would be highly desireable.

Acknowledgements–The NASA 1998 Leonid MAC was made possible by a number of individuals and organizations (see Jenniskens *et al.*, 1999 for a more complete list of these individuals and organizations). The SETI Institute and NASA Ames funded and coordinated the experiment, U.S. Air Force 452nd Flight Test Squadron at Edwards AFB provided technical support. In particular, we would like to thank the FISTA crew, Joe Kristl, Sandy Nierman, Thomas Hudson, Andrew LeBlanc, Amy Fisher, Margaret Campbell; and Mount Allison University. The meteor image lab at Mount

Allison is supported by the Canadian Natural Sciences and Engineering Research Council.

Editorial handling: D. W. G. Sears

REFERENCES

ARLT R. (1998) Bulletin 13 of the International Leonid Watch. *WGN: J. Inter. Meteor Org.* **26,** 239–248.

BEECH M. (1984) The structure of meteoroids. *Mon. Not. R. Astron. Soc.* **211,** 617–620.

BEECH M. (1986) The Draconid meteoroids. *Astron. J.* **91,** 159–162.

BENYUKH V. V. (1974) Position of maximum brightness on meteor light curves. *Solar System Res.* **8,** 159–164.

BROWN P., SIMEK M., JONES J., ARLT R., HOCKING W. K. AND BEECH M. (1998) Observations of the 1996 Leonid meteor shower by radar, visual and video techniques. *Mon. Not. R. Astron. Soc.* **300,** 244–250.

CAMPBELL M. D. (1998) Light Curves of Faint Meteors: Implications for Physical Structure. B. Sc. honours thesis, Mount Allison University, Sackville, New Brunswick, Canada. 102 pp.

CAMPBELL M. D., HAWKES R. L. AND BABCOCK D. D. (1999) Light curves of faint shower meteors: Implications for physical structure. In *Meteoroids 1998* (eds. V. Porubcan and W. J. Baggaley), pp. 263–266. Slovak Academy of Sciences, Bratislava, Slovakia.

CEPLECHA Z., BOROVICKA J., ELFORD G. W., REVELLE D., HAWKES R., PORUBCAN V. AND SIMEK M. (1998) Meteor Phenomena and Bodies. *Space Sci. Rev.* **84,** 327–471.

CORRELL R. R., CAMPBELL M., LEBLANC A., WORDEN S. P., HAWKES R. L., MONTAGUE T. AND BROWN P. (1999) Electro-optical observational results of the 1998 Leonid shower. *Proc. 1999 AIAA Leonid Threat Conf.* 12 pp.

ELFORD W., STEEL D. AND TAYLOR A. (1997) Implications for meteoroid chemistry from height distribution of radar meteors. *Adv. Space Res.* **20,** 1501–1504.

FLEMING D. E. B., HAWKES R. L. AND JONES J. (1993) Light curves of faint television meteors. In *Meteoroids and Their Parent Bodies* (eds. J. Stohl and I. P. Williams), pp. 261–264. Slovak Academy of Sciences, Bratislava, Slovakia.

FUJIWARA V., UEDA M., SHIBA Y., SUGIMOTO M., KINOSHITA M., SHIMODA C. AND NAKAMURA T. (1998) Meteor luminosity at 160 km altitude from TV observations for bright Leonid meteors. *Geophys. Res. Lett.* **25,** 285–288.

FYFE J. D. D. AND HAWKES R. L. (1986) Residual mass from ablation of meteoroid grains detached during atmospheric flight. *Planet. Space Sci.* **34,** 1201–1212.

HAPGOOD M., ROTHWELL P. AND ROYVRIK O. (1982) Two station observations of Perseid meteors. *Mon. Not. R. Astron. Soc.* **201,** 569–577.

HAWKES R. L. AND JONES J. (1975) A quantitative model for the ablation of dustball meteors. *Mon. Not. R. Astron. Soc.* **173,** 339–356.

HAWKES R. L., HITCHCOCK P. E., FYFE J. D. D., DUFFY A. G. AND JONES J. (1987) Light curves of faint meteors (abstract). *Bull. Amer. Astron. Soc.* **19,** 751.

HAWKES R. L., MASON K. I., FLEMING D. E. B. AND STULTZ C. T. (1993) Analysis procedures for two station television meteors. *International Meteor Conference* **1992,** 28–43.

HAWKES R. L., CAMPBELL M. D., BABCOCK D. D. AND BROWN P. (1998a) The Physical Structure of Leonid Meteoroids: Evidence from Optical Observations. *Proc. 1998 AIAA Leonid Threat Conf.* 11 pp.

HAWKES R. L., BABCOCK D. D. AND CAMPBELL M. D. (1998b) *Analysis Procedures and Electro-Optical Results 1997 Leonid Campaign.* CRESTech internal publication contract 5FUSA-7-J151/001/SV, CRESTech Ltd., Toronto, Ontario, Canada. 57 pp.

JENNISKENS *ET AL.* (1999) The 1998 Leonid multi-instrument aircraft campaign. *Meteorit. Planet Sci.* **34,** 933–943.

JONES J. AND HAWKES R. L. (1975) Television observations of faint meteors: II. Light curves. *Mon. Not. R. Astron. Soc.* **171,** 159–170.

MCKINLEY D. W. R. (1961) *Meteor Science and Engineering.* McGraw-Hill, New York, New York, USA. 308 pp.

ÖPIK E. (1958) *Meteor Flight in the Atmosphere.* Interscience Publishers, London, U.K. 174 pp.

PIERS P. A. AND HAWKES R. L. (1993) An unusual meteor cluster observed by image intensified video. *WGN J. Inter. Meteor Org.* **21,** 168–174.

SIMONENKO A.N. (1968) Separation of small particles from meteor bodies. In *Physics and Dynamics of Meteors* (eds. L. Kresak and P. M. Millman), pp. 207–216. Springer-Verlag, New York, New York, USA.

STEEL D. (1998) The Leonid meteors: Compositions and consequences. *Astron. Geophys.* **39,** 24–26.

VERNIANI F. (1965) On the luminous efficiency of meteors. *Smithson. Contr. Astrophys.* **9,** 141–172.

Forward

Back

Table of Contents